Diaphragm-Type Mechanism for Passive Phase Shifting in Miniature PT Cryocooler

S. Sobol, G. Grossman

Technion – Israel Institute of Technology
Haifa, Israel 32000

ABSTRACT

A properly operating pulse tube (PT) cryocooler requires flow-to-pressure phase shifting at the hot end to provide close to zero phase within the regenerator and the cold heat exchanger. Typical optimum flow-to-pressure phase at the hot end is around -60 degrees; thus, the phase shifting mechanism should provide a distinct inertial behavior with a certain capability to dissipate acoustic power.

The most common method of creating the proper phase shift involves the use of an inertance tube (IT), a long and thin tube with a reservoir attached to its far end. However, as a PT cryocooler is scaled down, the IT efficiency degrades due to the rapid increase of the resistive fluid impedance. Additionally, miniaturization of the cryocooler is generally accompanied by an increase in the operating frequency, which, in turn, magnifies the ineffectiveness of the IT further. A combination of the IT with a bypass flow tubing is also not sufficient for adequate shifting of the flow-to-pressure phase in ultra-miniature PT cryocoolers.

In fact, the only available method of creating the proper phase in a miniature high-frequency PT cryocooler entails the use of a warm mechanical expander. We propose to construct an expander consisting of a passively oscillating mass suspended on soft silicone diaphragms, which are frictionless, to provide a perfect dynamic seal with ease of miniaturization, and to perform the necessary function of a viscous damper. The research includes an analytical model, numerical simulations and an actual prototype of the proposed phase shifting mechanism tested on our MTSa miniature PT cryocooler.

INTRODUCTION

In recent years, many efforts have been made worldwide to miniaturize a pulse tube (PT) cryocooler, while retaining an adequate cooling capacity at lowest possible temperature. The corresponding miniaturization should be accompanied by increasing the filling pressure, the pressure ratio and the operating frequency. R. Radebaugh in 2006 showed that a PT can theoretically be operate effectively at frequencies up to 1000 Hz with a screen type regenerator of 7 mm length only [1]. However, no one has been able to approach these values practically. One of the obstacles to the PT miniaturization is the inability to produce a proper flow-to-pressure phase shifting mechanism of the appropriate miniature size.

A properly operating PT cryocooler requires very little flow-to-pressure phase within the regenerator and the cold heat exchanger. The corresponding phase at the hot end is obtained at about -60°, which is equivalent to a phase of -150° of the gas travel relative to the pressure wave. The

Cryocoolers 19, edited by S.D. Miller and R.G. Ross, Jr.

phase much under -90° indicates a distinct inertial behavior of the planned phase shifting mechanism, which should also have a certain capability to dissipate acoustic power.

The most common passive method of the flow-to-pressure phase shifting involves the use of a inertance tube (IT), a long and thin tube with a reservoir attached to its far end. The IT is a very simple and reliable mechanism, which is also very effective in medium and large scale PT cryocoolers. However, as the PT is scaled down, the effectiveness of the IT degrades due to a rapid increase of the resistive fluid impedance, which is inversely proportional to the tube diameter to the 5th power, whereas the inertance component changes just as the 2nd power [2]. Additionally, the flow resistance increases further with the frequency, the filling pressure and the pressure ratio, while the inertance effect is independent on these parameters. As a result, the maximum flow-to-pressure phase that the IT is able to create drops to zero as the PT cryocooler is miniaturized while retaining a nominal cooling capacity. The combination of the IT with a bypass flow tubing may improve the phase by about 10 degrees, but it is definitely not sufficient for the proper operation of an ultra-miniature PT cryocooler.

In fact, to date the only available method of creating the proper phase in a miniature high-frequency PT cryocooler entails the use of a mechanical warm expander (WE). Active WE systems, employing the inversely operating pressure oscillator as a phase shifting mechanism were investigated in the past [3], [4]; however, this solution is expensive and hard to miniaturize. Passive WE systems were theoretically considered [3], [5]. We propose to implement a passive expander consisting of a pressure driven oscillating mass suspended on soft silicone diaphragms, which are frictionless, provide a perfect dynamic seal, are easy to miniaturize, and contribute to the required damping. Unlike the IT, the mechanical oscillator has no inherent size or frequency dependent restrictions. Therefore, a properly designed passive expander should be able to supply the required flow-to-pressure phase at any operational frequency regardless of the PT dimensions and pressure amplitude.

THEORY

Figure 1 demonstrates schematically the proposed passive warm expander (WE). The oscillating mass of the system consists of two pistons with cross sectional areas A_1 and A_2, linked together by a rigid heavy rod of mass m. The pistons partition the interior space of the system housing into three volumes: front volume (V_f), intermediate volume (V_i) and buffer volume (V_b). The corresponding absolute pressures within the volumes are given by P_f, P_i and P_b. The average pressure P_0 is uniform along the system and is equal to the filling pressure of the PT. The front volume is connected to the hot end of the PT through the transfer line, and must provide the proper flow phase and amplitude to the cryocooler.

The linked pistons are supported axially by a mechanical spring k_m, which allows axial displacement x relative to the equilibrium point. Since the spring is intended to represent the stiffness of elastomeric diaphragms, the hysteretic damping coefficient η is also taken into consideration. Piston A_2 includes apertures filled by porous material, which allow for the gas to flow from the buffer volume to the intermediate volume and vice versa with a certain pressure drop. A proper design of the gas passaging might supply a linear flow to pressure drop relation, which should result in creating a linear viscous damping mechanism within the system.

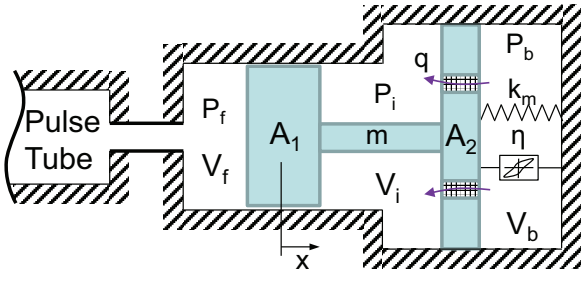

Figure 1. Schematic of the passive warm expander.

Linear Model of the Passive Warm Expander

The governing equations of the system are given by (1) and (2):

$$m\ddot{x} + k_m(1+i\eta)x = (P_f - P_i)A_1 + (P_i - P_b)A_2 \tag{1}$$

$$q = -C_V(P_i - P_b) \tag{2}$$

Where, $i = \sqrt{-1}$, q is the volumetric flow rate through the apertures in piston A_2, C_V is the linear flow coefficient. Under the assumption of small pressure ratios, the mass conservation equation within the adiabatic buffer volume can be expressed by (3) [6]:

$$-\frac{P_0}{RT_0}\mathbf{q} = \frac{V_{b0}\dot{\mathbf{P}}_\mathbf{b}}{\gamma RT_0} + \frac{P_0\dot{\mathbf{V}}_\mathbf{b}}{RT_0} \tag{3}$$

Where, γ is the adiabatic constant, R is the gas constant, and T_0 is the time average temperature.

Eq. (3) is given in vector notation, where the first term on the right hand side of (3) represents the mass accumulation within the volume, and the second term represents the volume change rate due to displacement of the pistons. All three vectors are assumed to be purely sinusoidal with a uniform angular velocity ω. In this case Eq. (3) can be simplified as follows:

$$-P_0\mathbf{q} = \omega\left(\frac{1}{\gamma}V_{b0}\mathbf{P}_\mathbf{b} + P_0\mathbf{V}_\mathbf{b}\right) \tag{4}$$

Where $\mathbf{P}_\mathbf{b}$ and $\mathbf{V}_\mathbf{b}$ are pressure and volume sinusoidal functions, substituted in (4) instead of their respective time derivatives in (3). Now, we would like to consider a very special case, where the pressure amplitude is about two orders of magnitude lower than the filling pressure, and, on the other hand, the volume amplitude is about half the mean buffer volume V_{b0}:

$$\begin{cases} \dfrac{|\mathbf{P}_\mathbf{b}|}{P_0} \sim 0.01 \\ \dfrac{|\mathbf{V}_\mathbf{b}|}{V_{b0}} \sim 0.5 \end{cases} \quad \Rightarrow \quad \left|\frac{1}{\gamma}V_{b0}\mathbf{P}_\mathbf{b}\right| \ll |P_0\mathbf{V}_\mathbf{b}| \tag{5}$$

In this special case the gas accumulation term in (3) is neglected relative to the volume change term, and thus can be omitted. As a result, the following algebraic relation for q is obtained:

$$q \approx -\dot{V}_b = A_2\dot{x} \tag{6}$$

Substitution (6) of (2) into provides a relation between the pressure drop on the A_2 piston and the piston velocity:

$$P_i - P_b = -\frac{A_2\dot{x}}{C_V} \tag{7}$$

Substitution of (7) into (1) provides the modified motion equation of the pistons:

$$m\ddot{x} + c\dot{x} + k_m(1+i\eta)x = (P_f - P_i)A_1 \tag{8}$$

Where:

$$c = \frac{A_2^2}{C_V} \tag{9}$$

The resulting relation (8) is actually a classic linear motion equation driven by oscillating pressure force, and having additional hysteretic damping. For the pressure given by (10), the piston displacement and the front volume magnitude can be expressed in general by (11) :

$$P_f - P_i = P_1\cos\omega t \tag{10}$$

$$\begin{aligned} x &= x_1\cos(\omega t + \theta) \\ V_f &= V_0 + V_1\cos(\omega t + \theta) \end{aligned}, \quad V_1 = A_1x_1 \tag{11}$$

where x_1 and V_1 are piston and volume amplitudes respectively, and θ is actually the gas travel-to-pressure phase. A general solution for the volume amplitude and the corresponding phase is the following:

$$\begin{cases} V_1 = \dfrac{P_1 A_1^2}{\sqrt{\left(\omega c + \eta k_m\right)^2 + \left(\omega^2 m - k_m\right)^2}} \\ \tan\theta = \dfrac{\omega c + \eta k_m}{\omega^2 m - k_m} \end{cases} \tag{12}$$

Matching the Passive Warm Expander to the PT Cryocooler

We consider a specific pulse tube cryocooler, designed to operate at a frequency $f_0=\omega_0/2\pi$ with a pressure amplitude P_1. A separate analysis of the PT shows that a phase shifting mechanism connected to the hot end should supply the swept volume amplitude of V_1 and the travel-to-pressure phase of θ_0 for achieving the proper PT operation. The phase shifting mechanism is implemented by a passive WE described schematically in Figure 1, and the WE oscillations are governed by Eq. (12). The pistons are suspended on elastic diaphragms, which possess total axial stiffness k_m and the corresponding hysteretic damping coefficient ηk_m. Cross sectional areas of the pistons can be chosen arbitrarily.

The first objective refers to estimation of a mass and a viscous damping coefficient as a function of A_1, k_m and η, which would create the proper dynamics of the WE matching the PT requirements. For this purpose, Eq. (12) should be solved for m and c, while it is known in advance that θ_0 should be below -90°. The appropriate solution is given by Eq. (13):

$$\begin{cases} m = \dfrac{k_g + k_m}{\omega_0^2} \\ c = \dfrac{k_g \left|\tan\theta_0\right| - \eta k_m}{\omega_0} \end{cases}, \quad -180° < \theta_0 < -90° \tag{13}$$

Where:

$$k_g = \frac{P_1 A_1^2 \left|\cos\theta_0\right|}{V_1} \tag{14}$$

One should notice that the stiffness k_g defined in (14) is actually the PT gas stiffness measured on the A_1 piston boundary.

In order to verify the results obtained in (13), we first modified the SAGE™ model of our MTSa miniature PT cryocooler [7] for operating with a passive piston instead of the original IT system. Figure 2 partially demonstrates a root level of the SAGE™ model, where the bottom row components represent the structure of the passive expander. The schematic of the SAGE model expander differs from the one shown in Figure 1 by the absence of the secondary piston A_2. Instead, there is a single buffer volume and a linear damper connected in parallel to the oscillating mass and the mechanical spring as shown in Figure 2 in a separate window.

MTSa [7] was designed to operate at 100 Hz with a filling pressure of 40 bar and a pressure ratio of 1.3. Due to the pressure drops along the cryocooler, the average pressure amplitude within the hot heat exchanger is obtained at 4.45 bar. According to previous simulations we know that the optimum swept volume amplitude and the travel-to-pressure phase at the hot end should be 23.6 mm^3 and -145°, respectively.

We chose a passive piston of 5 mm diameter, which should result in a 1.2 mm piston amplitude, k_m = 3 N/mm and η = 0. In this case the gas stiffness is obtained at 5.95 N/mm according to (14). According to (14), the oscillating mass and the damping coefficient should be 22.5 g and 6.8 N/m, respectively. These analytically obtained parameters (A_1, m, c and k_m) were substituted into the SAGE model, which was run at various frequencies while retaining the nominal pressure amplitude at the hot end. The resulting piston amplitude and phase are shown in Figure 3 together with the analytical frequency response. It can be clearly seen that both the analytical and the SAGE models satisfy perfectly the required 1.2 mm amplitude and -145° phase at 100 Hz.

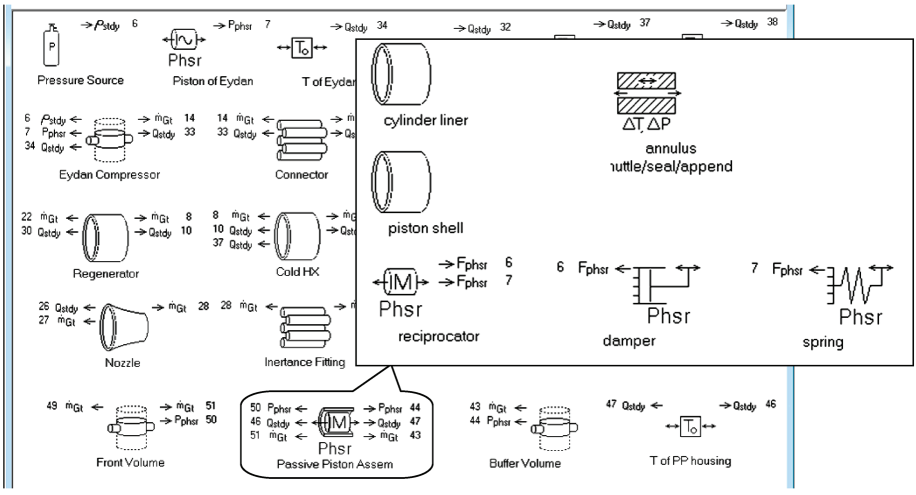

Figure 2. SAGE model of the MTSa PT with a passive warm expander.

PRELIMINARY PROTOTYPE

Viscous Damping Mechanism

Implementation of the viscous damper is based on Eq. (9), and should not violate the conditions given in (5). A linear flow-to-pressure-drop relation can be achieved using mesh stacks with sufficiently small gas passages, which ensure a laminar flow regime. A suitable candidate was found in a random fiber stainless steel mesh of 0.4 mm thickness with a porosity of 0.75. The mesh was cut into discs of 2 mm diameter for further arrangement within the A_2 apertures. Figure 4 shows the enlarged disk illustration together with a measured flow capacity of a single disk, where the examined fluid was pure nitrogen at room conditions. According to the figure, the flow curve is perfectly linear for pressure drops up to 0.3 bar at least, where the flow reaches 2.5e-5 m^3/s. The linear flow coefficient of a single disk is estimated at 8.4334e-10 $(m^3/s)/Pa$.

Because of some design constrains, the effective diameter of the secondary piston A_2 was set to 14 mm. According to Eq. (6) the maximum flow rate at 100 Hz with the piston amplitude of 1.2 mm is estimated at 1.16e-4 m^3/s. This value exceeds by about four times the linear flow range of a single disk; hence, in order to ensure small pressure drops, at least four single disks should be ar-

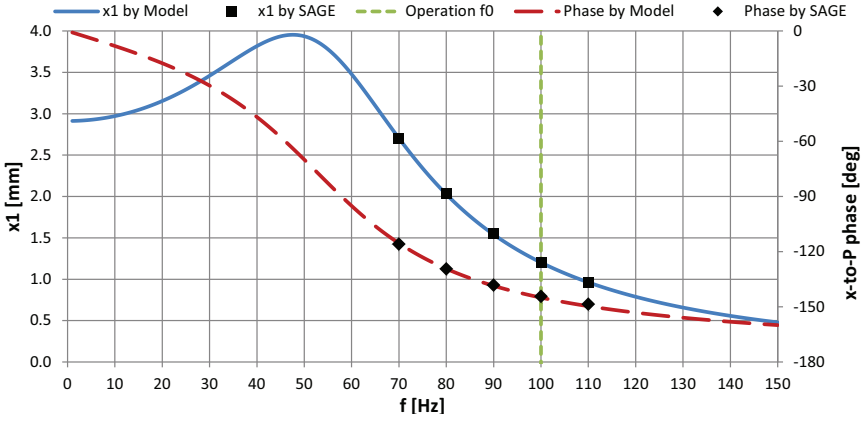

Figure 3. SAGE™ vs. analytical model frequency response.

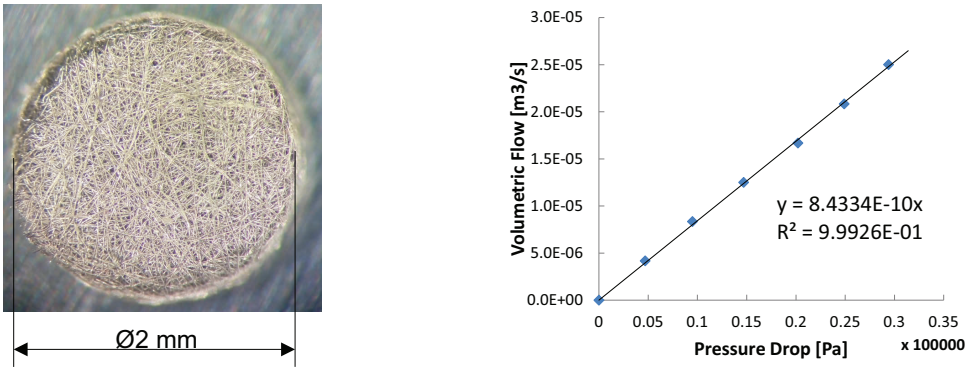

Figure 4. Illustration and flow capacity of a single random mesh disk.

ranged across the A_2 piston in parallel. According to Eq. (9), arrangement of four disks in parallel should result in 7.0 N/m for the viscous damping coefficient. In the previous section of the paper we considered a case where the required viscous damping in the absence of the hysteresis was estimated at 6.8 N/m, which is quite close to the value obtained here.

CAD Model

Figure 5 demonstrates exploded and section views of the preliminary WE assembly. The A_1 and A_2 pistons are molded together with the corresponding cylinders by 25 shore-A adhesive silicone. The pistons and the cylinders were machined with patterns of small apertures for enlarging the contact areas, thus improving the silicone to metal adhesion. The mutual axis was tapped by M2 thread for simplicity in fastening of the mass element, the A_2 piston and the mirror located on the right hand end of the axis. The mirror is utilized for the real time measurement of the axial displacement using an external laser-detector system. The buffer volume of the housing is covered by a glass window, which allows the laser beam to pass freely in both directions regardless of the

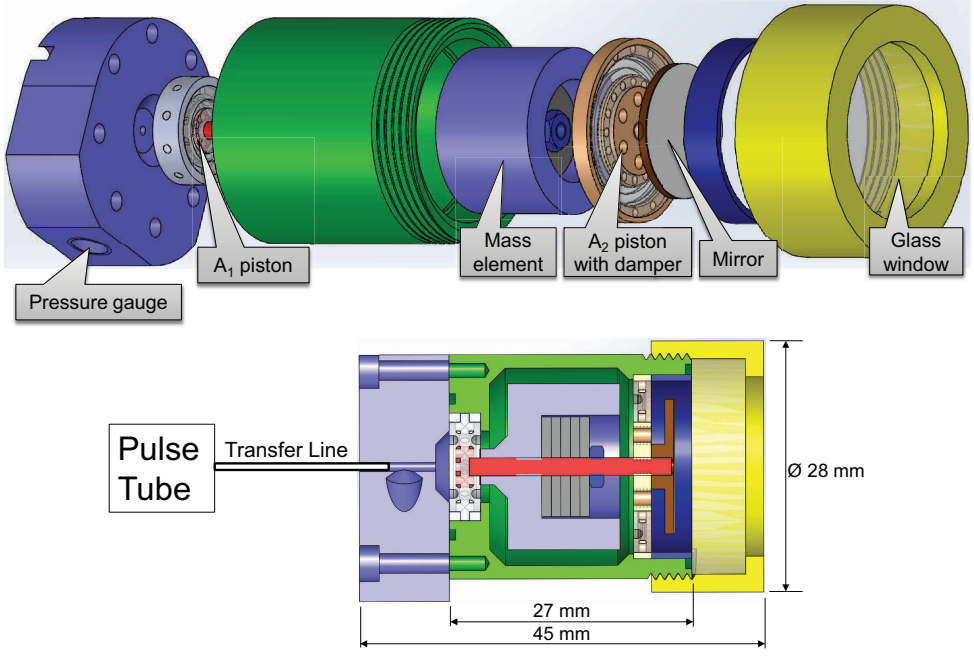

Figure 5. CAD model of the preliminary warm expander.

axis instantaneous location. The front side of the housing is covered by a thick flange for allowing pressure gauge installation.

The total length of the WE system is 45 mm. The length can be decreased by about 10 mm with the pressure and displacement measurement systems eliminated. In this case the overall size of the WE housing would be dictated mostly by the mass element dimensions. According to Eq. (13) the mass and its corresponding dimensions are intended to decrease as the operating frequency increases and/or as the silicone diaphragms create lower axial stiffness. Currently, the oscillating mass is adjustable between 24 and 32 gram according to the number of the lead disks added to the main mass element.

Silicone Diaphragms

Advantages of the diaphragm type suspensions over the commonly used gas-gap sealing methods are the following: they provide frictionless motion, are a perfect dynamic seal, are easy to miniaturize, and do not require high precision and assist in damping due to the natural hysteresis of polymers. Additionally, well treated silicones possess very good temperature stability and produce very little outgassing. On the other hand, the diaphragms may produce the enhanced axial stiffness; the effective diameter may vary with the pressure drop; fatigue problem is more topical; and the non-linear effects are quite significant. The influence of the latter is magnified while operating in the vicinity of the resonance frequency; however, the non-linear effects can be reduced drastically by applying sufficient damping on the oscillator.

Figure 6 demonstrates an example of a numerical simulation of the A_1 piston diaphragm, where the piston is displaced downwards by 1 mm, and pressure of 4 bar is applied on the bottom surfaces. Mechanical properties of the silicone were specified by hyper elastic Neo-Hookean material model with an initial shear modulus of 0.22 MPa and the incompressibility parameter of 17.7 GPa^{-1}. The maximum equivalent strain was obtained at 77.7%, while the maximum allowable strain of the specific silicone should exceed 300%. The equivalent piston diameter is obtained at 5.4 mm. No-pressure simulation of the diaphragm provided estimation of the axial stiffness, which was obtained increasing from 4.4 to 4.7 N/mm as a function of the piston displacement.

Experiment Setup

A preliminary prototype of the proposed passive WE has been constructed and connected to our miniature MTSa PT cryocooler through 0.7 mm inner diameter, 100 mm length transfer line. Figure 7 illustrates the experimental setup, with the WE installed vertically, and the front volume rotated upwards. The WE housing shares a rigid basis with a travel measurement system, consisting of a laser module and a Position Sensitive Detector (PSD) unit. Both are adjustable for a proper angle and location relative to the mirror within the WE housing.

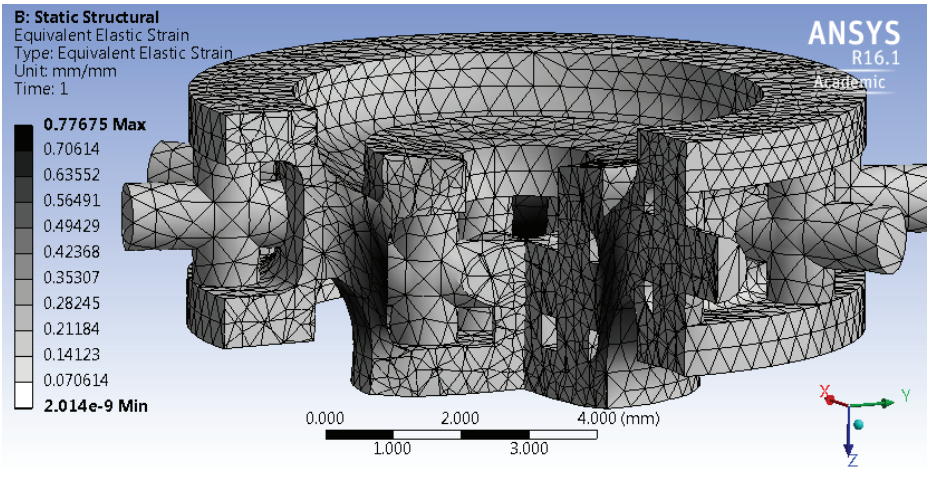

Figure 6. Simulation on A_1 piston diaphragm with $\Delta x = 1$ mm, $\Delta P = 4$ bar.

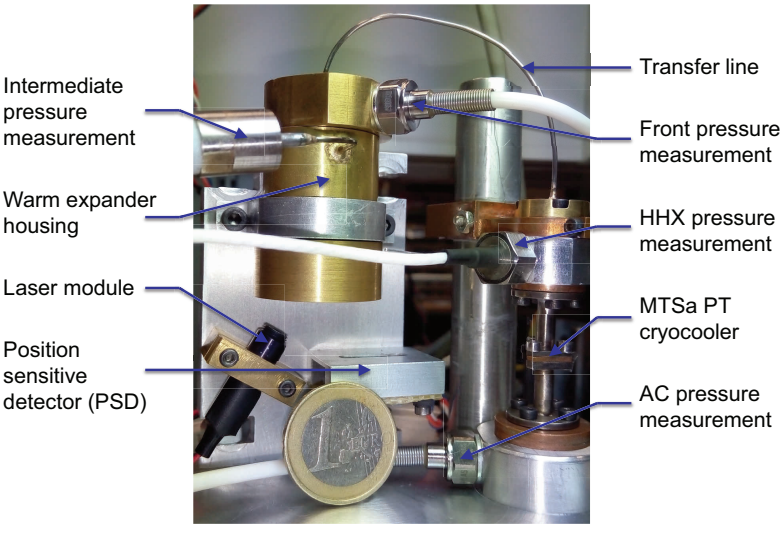

Figure 7. Experiment setup.

Four pressure gauges are installed along the PT-WE system: in the aftercooler, in the hot heat exchanger, in the front and the intermediate volumes of the WE. The pressure wave is supplied by a pressure oscillator located under the illustrated setup, outside the vacuum chamber.

RESULTS AND DISCUSSION

The experiments were conducted with the mass element set to the maximum possible 32 g due to the enhanced axial stiffness of the silicone diaphragms obtained after the molding. The total static axial spring constant due to both diaphragms elasticity was estimated at about 12 N/mm, while the initial prediction based on numerical simulations was about 8 N/mm. The viscous damping mechanism included six random fiber disks, as described previously, in parallel arrangement. Pressure ratio at the front volume of the WE system was retained for all the examined frequencies at nearly 1.1, which is equivalent to 1.85 bar amplitude over the filling pressure of 40 bar.

Figure 8 (top row) summarizes piston amplitudes and phases relative to the pressure difference on A_1 at various operating frequencies. The smooth curves represent the best fit theoretical model response according to Eq. (8). It can be clearly seen that at least one additional motion mode was excited at 130 Hz in the experiment. The mode has distorted the predicted amplitude curve; however, it had a minor effect on the phase. Apparently, the phase response should provide more reliable information on the axial travel mode than the amplitude.

The phase response curve crosses -90° at 102 Hz, which should be the natural frequency of the axial motion. Therefore, taking into account the oscillating mass of 32 g, the effective dynamic spring constant k_m is estimated at 13 N/mm, which is about 8% larger than the measured static stiffness. Since the hysteretic damping constant of the utilized silicone was estimated previously at about 0.1, the only underestimated parameter in Eq. (8) remained the viscous damping coefficient. The best fit between the theoretical model and the measured data was obtained for $c = 6.5$ Ns/m, which is quite close to the one obtained in the previous chapter of the paper despite a different fluid and different pressure.

A bottom row of plots in Figure 8 shows the time scaled measurements of the pistons travel and the appropriate pressures at the frequency of 140 Hz, which provided a phase lag of 145° required for operation of our MTSa PT cryocooler. Certainly, this frequency is too distant from the nominal 100 Hz, and the amplitude at 140 Hz is still affected by the undesired mode; thus it is unreasonable to conduct the cooling capacity experiments on MTSa at these conditions. One should notice that

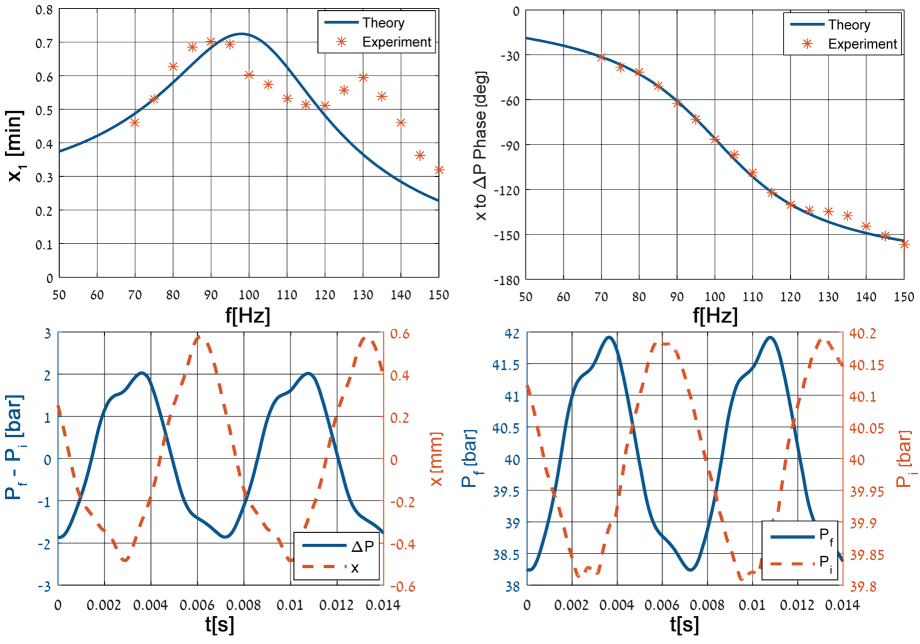

Figure 8. Top – Frequency response of the prototype and the corresponding theoretical model; Bottom – Measured pressures and displacement at 140 Hz.

the intermediate pressure P_i is obtained with about ten times lower amplitude than that of the front pressure P_f, and, therefore, has a minor effect on x-to-P_f phase and the pressure force applied on A_1 piston.

SUMMARY AND CONCLUSIONS

A simplified analytical model was developed for designing a passive warm expander (WE), with the intention to provide a proper flow-to-pressure phase shifting for PT cryocoolers regardless of the PT size, operating frequency and pressure ratio. The model estimates the mass and damping coefficient values for the WE oscillator as functions of the arbitrarily chosen spring constant, the passive piston diameter and the PT requirements. The viscous damping is determined by the secondary piston diameter and the linear flow coefficient obtained from the gas flow capacity through the secondary piston apertures.

The analytical model demonstrated a perfect agreement with the SAGE™ model, where the damping mechanism was not implemented entirely but represented by artificial viscous damping component with a constant coefficient. The models have verified that our MTSa PT cryocooler operating at 100 Hz with pressure ratio 1.3 requires for optimum operation the WE oscillator of 23.5 gr with damping coefficient of 6.8 Ns/m, when the passive piston diameter is set to 5 mm and the spring constant is 3 N/mm.

A preliminary prototype of the passive WE system was designed, fabricated and tested at various frequencies. The overall dimensions of the WE system are Ø28x45 mm, where about 10 mm of the length are extraneous due to pressure and displacement measurement systems. The prototype includes two rigidly linked pistons of 5.4 and 14.0 mm diameters suspended on silicone diaphragms, a mass element of 32 gr, and viscous damping mechanism, which produces a linear damping coefficient of 6.5 Ns/m.

The WE prototype proved the ability to create any flow-to-pressure phase appropriate for a PT cryocooler. The implemented viscous damping mechanism demonstrated a good agreement with the

theoretical model. Furthermore, the actual damping coefficient is amenable to easy tuning by changing the amount and/or the arrangement of the mesh disks within the apertures across the A_2 piston.

Unfortunately, several technical drawbacks did not enable perfect matching between the WE system and our MTSa PT cryocooler. First, material properties of the silicone utilized for the diaphragms were estimated inaccurately; thus, the total measured axial spring constant was about 60% larger than the calculated one. Additional stiffness increase was obtained in dynamic operation due to the pressure drop applied on the secondary piston and the total gas compressibility in the intermediate and the buffer volumes. Finally, the axial spring constant turned out almost twice larger than the required one for the 32 gram mass, and, as a result, the natural frequency of the oscillator was shifted by a factor of 1.4. Consequently, the desired -145° of travel-to-pressure phase was obtained at 140 Hz instead of at the nominal 100 Hz.

The second drawback refers to excitation of additional motion modes of the oscillator in the vicinity of the operating frequencies. At least one parasitic mode was detected at 130 Hz; however, it affected the measured amplitudes in a wide range around. Obviously, the WE system requires a full modal analysis and a subsequent dynamic redesign, which would shift the undesired modes far away from the operational range of frequencies.

ACKNOWLEDGMENT

The generous financial support of the Rechler Family, MAFAT and the Technion is gratefully acknowledged.

REFERENCES

1. Radebaugh, R. and O'Gallagher, A., "Regenerator operation at very high frequencies for microcryocoolers," *Adv. in Cryogenic Engineering*, Vol. 51, Amer. Institute of Physics, Melville, NY (2006), pp. 1919-1928.
2. Radebaugh, R., Lewis, M., Luo, E., Pfotenhauer, J.M., Nellis, G.F. and Schunk, L.A., "Inertance Tube Optimization for Pulse Tube Refrigerators," *Adv. in Cryogenic Engineering*, Vol. 51, Amer. Institute of Physics, Melville, NY (2006), pp. 59-67.
3. Brito, M.C. and Peskett, G.D., "Experimental Analysis Of Free Warm Expander Pulse Tube," *Cryogenics,* vol. 41 (2001), pp. 757–762
4. Lewis, M., Bradley, P. and Radebaugh, R., "Experiments With Linear Compressors For Phase Shifting In Pulse Tube Crycoolers," *Adv. in Cryogenic Engineering*, Vol. 57, Amer. Institute of Physics, Melville, NY (2012).
5. Zhu, S. and Nogawa, M., "Pulse Tube Stirling Machine with Warm Gas-Driven Displacer," *Cryogenics,* vol. 50 (2010), pp. 320–330.
6. Radebaugh, R., "A Review of Pulse Tube Refrigeration," *Adv. in Cryogenic Engineering*, vol. 35, Springer US (1990), pp. 1191-1205.
7. Sobol, S., Katz, Y. and Grossman, G., "A Study Of A Miniature In-Line Pulse Tube Cryocooler," *Cryocoolers 16*, ICC Press, Boulder, CO (2011), pp. 87-95